Anomalous thermodynamic properties and phase stability of δ-$Pu_{1-x}M_x$ (M=Ga and Al) alloys from first-principles calculations

Chun-Mei Li,[1,2,*] Rui Yang,[2] Börje Johansson,[3,4,5] and Levente Vitos[3,4,6]

[1]*College of Physical Science and Technology, Shenyang Normal University, Shenyang 110034, China*

[2]*Shenyang National Laboratory for Materials Science, Institute of Metal Research, Chinese Academy of Sciences, 72 Wenhua Road, Shenyang 110016, China*

[3]*Applied Materials Physics, Department of Materials Science and Engineering, Royal Institute of Technology, Stockholm SE-100 44, Sweden*

[4]*Condensed Matter Theory Group, Physics Department, Uppsala University, P.O. Box 516, SE-75120 Uppsala, Sweden*

[5]*School of Physics and Optoelectronic Technology & College of Advanced Science and Technology Dalian University of Technology, Dalian 116024, China*

[6]*Research Institute for Solid State Physics and Optics, Budapest H-1525, P.O. Box 49, Hungary*

(Received 27 September 2016; revised manuscript received 21 November 2016; published 16 December 2016)

The composition-dependent crystal structure, volume, elastic constants, and electronic structure of δ-$Pu_{1-x}M_x$ (M = Ga and Al, $0 \leqslant x \leqslant 0.1$) alloys are systematically studied by using first-principles EMTO-CPA calculations. It is shown that the fcc and $L1_2$ structures co-exist in the alloys with $x \leqslant 0.04$ whereas for $x > 0.04$, the $L1_2$ structure is more and more preferable and around $x = 0.1$, it tends to be stabilized alone. The evaluated $V \sim x$ of the $L1_2$ structure, being negative deviation from Vegard's law, turns out to be in good agreement with the experimental result. For $x \leqslant 0.04$, the estimated E, G, ν, and Θ of both the fcc and $L1_2$ structures are in line with the measured data, whereas when $x > 0.04$, only those of the $L1_2$ structure are close to the experimental results. The electronic hybridization between Pu and M atoms is dominated by Pu for the s, d, and f states but M for the p state. The strong interactions between Pu and M atoms in the same site of the $L1_2$ structure should be responsible for its relative stability in the alloys with $x > 0.04$. The electron-phonon coupling further decreases the phase stability of δ-$Pu_{1-x}M_x$ with increasing x.

DOI: 10.1103/PhysRevB.94.214108

I. INTRODUCTION

As one of the most exotic elemental metals, plutonium (Pu) exhibits six complex solid-state phases before melting at 923 K [1–5]. Understanding all the six allotropic phases is crucial to the safe handling, use, and long-term storage of this technologically important material [5,6]. The face-centered-cubic (fcc) δ phase, which is stable between 592 and 724 K, when alloyed with a small amount of Al, Ga, Ce, or In, can be even stabilized or retained below room temperature and possess desirable mechanical properties, such as good ductility that allows it to be formed into complicated shapes [7,8]. The δ-Pu based binary alloys thus especially attract a lot of research.

The different alloying elements M in δ-$Pu_{1-x}M_x$ have different composition ranges of δ stabilization or retention. The Ga-alloying stabilizes the δ phase with its concentration (x) varying from 0.01 to 0.125 [4,9], whereas the Al alloying does so with x changing from 0.025 to 0.11 [10,11]. With more Ga/Al addition, these δ-$Pu_{1-x}M_x$ alloys generally decompose into a mixture of $\delta + Pu_3Ga/Pu_3Al$ above the room temperature, with Pu_3Ga/Pu_3Al possessing an approximate $L1_2$ structure [11–13]. The δ stabilization is therefore expected to be correlated with the composition-dependent site occupation of the M atoms as well. It has been probed recently by the extended x-ray absorption fine structure (EXAFS) spectroscopy that in δ-$Pu_{1-x}Ga_x$, the Ga atoms rigorously avoid bonding to each other even at relatively high concentrations, where they nevertheless interact over longer distances [14]. However, until now, the composition-dependent site preference of the M atoms is still not deeply understood.

Most recently, new neutron-scattering experiments and phonon dispersion calculations have shown that the δ-Pu phase contains magnetism and its magnetic form factor has been derived [15,16], which provides a new powerful proof for its so many successful theoretical studies with the approximated paramagnetic (PM) state [17–19], since no static local magnetic moment in Pu was supposed ten years ago [20]. In the present calculations, δ-$Pu_{1-x}M_x$ is approximated to be in the PM state as well, described with the fully disordered local magnetic (DLM) model [21]. At high temperature, the spin fluctuations could induce both strong magnetovolume and magnetoelasstic couplings in δ-Pu [22]. Similarly, in δ-$Pu_{1-x}M_x$ alloys, the site preference of the alloying element M varies the local environments of the Pu atoms, and then changes their local electronic distribution, which could be supposed to consequently influence the volume, elastic moduli, and also the phase stability of these alloys.

To build the connection between the composition and the thermodynamical properties as well as the phase stability, and then to understand their underlying physics are critical for designing δ-$Pu_{1-x}M_x$ alloys with desirable mechanical properties. In this paper, we will systematically explore the composition-dependent crystal structure, volume, elastic properties, and electronic structure including the electron-phonon coupling effect of δ-$Pu_{1-x}M_x$ (M = Ga and Al, $0 \leqslant x \leqslant 0.1$) alloys, and then try to get their physical mechanism and their correlation with the phase stability. The rest of the paper is arranged as follows: in Sec. II, we describe the first-principles method we used and the calculation details; in Sec. III, the composition-dependent crystal structure, volume, elastic

*Corresponding author: cmli@synu.edu.cn

constants, and electronic structure are presented, and their relationship with the phase stability are discussed. Finally, we summarize the main results of this work in Sec. IV.

II. METHODS AND CALCULATION DETAILS

Based on density functional theory, the employed first-principles solver is the exact muffin-tin orbitals (EMTO) method [23,24], where the one-electron Kohn-Sham equation is solved by the use of a scalar-relativistic Green's function technique. The one-electron potential is represented by optimized overlapping muffin-tin potential spheres. The total energy is corrected with the so-called full charge-density (FCD) method [24]. In combination with the coherent potential approximation (CPA) [25–27], the EMTO-CPA method has been one of the few possible approaches to deal with both the chemical and magnetic disorder at the first-principles level. It has been now applied successfully in the study of the thermophysical properties and the spin fluctuation effect of metals and metallic alloys [23,25,27–30].

For the present application, the exchange correlation is chosen to be generalized gradient approximation (GGA) as described by Perdew, Burke, and Ernzerhof (PBE) [31]. The EMTO basis sets include s, p, d, and f components, and the scalar-relativistic and soft-core approximations are adopted. The Green's function is calculated for 32 complex energy points distributed exponentially on a semicircular contour. For the slope matrix, two-center Taylor expansion is used because of the wide bands of Pu, and the number of orbitals is truncated at eight. The Brillouin zone is sampled by a $13 \times 13 \times 13$ uniform k-point mesh without any smearing technique.

The crystal structures of δ-$Pu_{1-x}M_x$ alloys are considered two types. One is that the M and Pu atoms occupy commonly each site of a fcc lattice with the ratio of $x : 1-x$. Shown in Fig. 1(a), it is still a fcc structure. The another one is that the rich Pu atoms alone occupy the face-centered positions of the fcc lattice (called Pu1 atoms), whereas the M together with the left Pu atoms (named Pu2 atoms) co-occupy the vertexes of the cubic lattice with the ratio of $4x : 1-4x$. Described in Fig. 1(b), it turns out to be a $L1_2$ structure: (0, 0, 0) is occupied by Pu and M atoms, $(0, \frac{1}{2}, \frac{1}{2})$, $(\frac{1}{2}, 0, \frac{1}{2})$, and $(\frac{1}{2}, \frac{1}{2}, 0)$ are Pu atoms.

For both the fcc and $L1_2$ structures, the equilibrium volume (V) and bulk modulus (B) are determined by fitting the calculated 0 K electronic energies versus volume to a Morse function [32]. The 0-K single crystal elastic constants C' $((C_{11}-C_{12})/2)$ and C_{44} are evaluated with the same mathematical methods shown in our previous paper [33]. The elastic moduli of δ-$Pu_{1-x}M_x$ alloys strongly soften with increasing T [34,35]. In order to facilitate the comparison between their static values with the measured ones at high temperature, the lower bounds of the Hill average, i.e., the Reuss averaging method is adopted to calculate these 0-K polycrystal elastic constants [24].

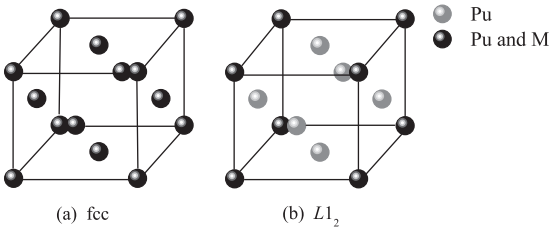

FIG. 1. Unit cells of δ-$Pu_{1-x}M_x$ alloys with the face-centered-cubic (fcc) (a) and simple cubic $L1_2$ (b) structures, respectively. The gray spheres denote the sublattices occupied by Pu atoms alone, whereas the black spheres describe the sublattices occupied by a mixture of Pu and M atoms.

The formation energy (E_f) of δ-$Pu_{1-x}M_x$ system is defined as

$$E_f = E_{\text{tot}} - (1-x)E_{\text{Pu}} - xE_M + TS_{\text{mix}}, \tag{1}$$

with E_{tot} being the total energy per atom of the unit cell, E_{Pu} and E_M the total energies per atom of Pu and M in a fcc lattice, respectively, and TS_{mix} $[= k_B T(x \ln x + (1-x)\ln(1-x))]$ the chemical mixing entropy of the alloy. Here, all the E_{tot}, E_{Pu}, and E_M include the electronic total energy and electronic entropy two parts. For the static electronic total energy (E_{el}) and static electronic entropy ($-TS_{\text{el}}$) terms, they are calculated directly with the EMTO-CPA tool. The S_{el} is evaluated with

$$S_{\text{el}} = -2k_B \int_{\infty}^{\infty} \{f(E)[\ln f(E)] + [1-f(E)]\ln[1-f(E)]\} N(E) dE, \tag{2}$$

with $N(E)$ being the static density of states (DOS), and k_B the Boltzmann constant [36].

For real metals at elevated temperature, the electrons experience a smeared DOS $[N^*(E)]$ as a result of phonon-limited lifetime. This effect can be formulated as a Lorentz-type smearing of the static DOS,

$$N^*(E) = \int_{\infty}^{\infty} N(\varepsilon) \frac{(\Gamma/\pi)}{(E-\varepsilon)^2 + \Gamma^2} d\varepsilon, \tag{3}$$

with Γ being inverse proportional with the electron lifetime, estimated with $\Gamma = \pi \lambda_{\text{el-ph}} k_B T$ [36]. Here, the electronic-phonon coupling parameter, $\lambda_{\text{el-ph}}$, is taken to be 0.8 [37]. The electronic temperature, T, equals to 700 K. Replacing $N(E)$ in Eq. (2) with $N^*(E)$, we get the smeared electronic entropy ($-TS^*_{\text{el}}$) as well as the smeared electronic total energy (E^*_{el}) terms at finite temperature. As a result, the formation energy including the phonon-smearing (E^*_f) is obtained according to Eq. (1), and then the electron-phonon coupling effect on the phase stability of δ-$Pu_{1-x}M_x$ alloys is examined.

III. RESULTS AND DISCUSSIONS

A. Crystal structure

Figure 2 shows the x dependence of the E_f of δ-$Pu_{1-x}M_x$ [M = Ga in Fig. 2(a) and M = Al in Fig. 2(b), $0 \leqslant x \leqslant 0.1$] alloys with the fcc and $L1_2$ structures, respectively. At 0 K, the calculated E_f of the fcc structure first decreases and then increases with x, whereas the present E_f of the $L1_2$ structure decreases monotonically with increasing x in each group of alloys. When the static electronic entropy term, $-TS_{\text{el}}$, is taken into account at electronic temperature $T = 700$ K, the estimated E_f is still similar to that evaluated at 0 K for each alloy. For the two cases, the obtained minimum value of the E_f of the fcc structure always appears around $x = 0.07$ for

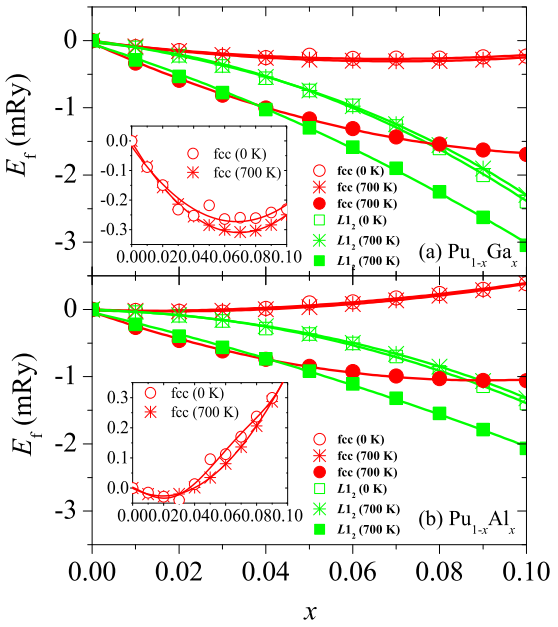

FIG. 2. x dependence of the formation energies (E_f) of δ-$Pu_{1-x}M_x$ [M = Ga (a) and Al (b), $0 \leqslant x \leqslant 0.1$] alloys with the fcc and $L1_2$ structures, respectively. The open and solid symbols denote the E_f at 0 and 700 K, respectively, whereas the stars mean the E_f calculated with Eq. (1) without the chemical mixing entropy term at 700 K.

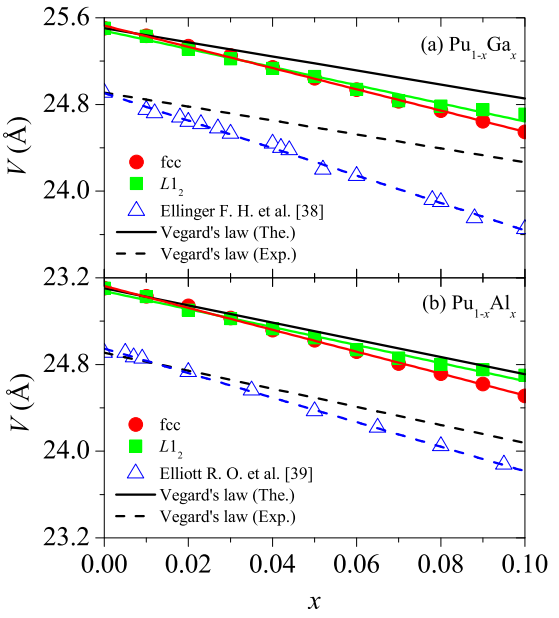

FIG. 3. x dependence of the equilibrium volume (V) of δ-$Pu_{1-x}M_x$ [M = Ga (a) and Al (b), $0 \leqslant x \leqslant 0.1$] alloys with the fcc and $L1_2$ structures, respectively, in comparison with the experimental results from Refs. [38,39], as well as those evaluated with the present V of the fcc M and the experimental (Exp.) and theoretical (The.) V of δ-Pu, respectively, according to Vegard's law [8].

M = Ga and $x = 0.03$ for M = Al alloy, as shown in the insert figures of Figs. 2(a) and 2(b), respectively. The static electronic entropy has practically no influence on the phase stability of these alloys.

When the chemical mixing entropy, TS_{mix}, is further added at 700 K, the evaluated E_f for each binary alloy gets to be much lower than its correspondent at 0 K. With increasing x, it goes down monotonically in both the fcc and $L1_2$ structures of each family, shown in Figs. 2(a) and 2(b), respectively. For $x \leqslant 0.04$, the E_f of the fcc structure tends to be lower than that of the $L1_2$ one merely less than 0.05 mRy at each x, meaning that the two crystal structures may coexist in these δ-$Pu_{1-x}M_x$ alloys. When $x > 0.04$, the E_f of the $L1_2$ structure changes to be lower than that of the fcc one, and with increasing x, this phenomenon is shown more and more evidently. When $x = 0.1$, the difference of E_f between the $L1_2$ and fcc structures even reaches about -1.35 mRy for M = Ga and -1.01 mRy for M = Al alloys. For $x > 0.04$, the $L1_2$ structure gets more and more stable than the fcc one with increasing x and around $x = 0.1$, it is expected to be stabilized alone in each group of alloys. This result provides a good understanding for the experimental finding that with increasing x up to around 0.1, δ-$Pu_{1-x}M_x$ alloys generally decompose into $\delta + Pu_3M$ above the room temperature, with Pu_3M having an approximate $L1_2$ structure (the c/a being slightly larger than 1) [11–13].

B. Volume

The x dependence of the V of δ-$Pu_{1-x}M_x$ (M = Ga and Al) alloys with the fcc and $L1_2$ structures, respectively, are shown in Fig. 3, in comparison with the available experimental data [38,39] as well as the results evaluated according to Vegard's law [8]. Shown in Figs. 3(a) and 3(b), respectively, the evaluated V of both M = Ga and Al alloys decrease monotonically with increasing x in each structure. For M = Ga shown in Fig. 3(a), the average slopes ($\frac{dV}{dx}$) of the curves of V versus x are about -9.8 for the fcc structure and -8.5 for the $L1_2$ one. For M = Al shown in Fig. 3(b), they tend to be -10.1 and -8.2, respectively. As well as the previous EMTO calculations [34], the present V of δ-Pu (25.5 Å) is a little larger than the measured data (25.0 Å) at high temperature [40]. This results in that both the estimated V and $\frac{dV}{dx}$ of these binary alloys turn out to be also a little larger than their experimental ones [38,39]. It deserves to be noted that the experimental $\frac{dV}{dx}$ of δ-$Pu_{1-x}Ga_x$ (-12.7) is a little smaller than that of δ-$Pu_{1-x}Al_x$ (-11.3), i.e., the decrease of V with the Ga doping is faster than that with the Al addition, although the atomic radius of the Ga is larger than that of the Al [38,39]. Here, the evaluated $\frac{dV}{dx}$ of M = Ga alloys with the $L1_2$ structure (-8.5) is smaller whereas that of the alloys with the fcc one (-9.8) is a little larger than those corresponding to M = Al alloys (-8.2 and -10.1, respectively). Seen from the whole composition range, the $L1_2$ structure is thus confirmed again to be more preferable than the fcc one.

According to Vegard's law [8], the V of δ-$Pu_{1-x}M_x$ is written with $V = (1-x)V_{\text{Pu}} + xV_M$, with V_{Pu} and V_M being the volume per atom of Pu and M, respectively, with the fcc structure. Since the fcc Ga is not available experimentally, the present V_M is always used whereas the estimated and measured V_{Pu} [38,39] are adopted here for the evaluations of the so-called theoretical and experimental V, respectively, according to the law. Shown in Figs. 3(a) and 3(b), as well as the experimental measurements [38,39], the calculated V versus x indeed turn out to be negative deviation from the evaluated

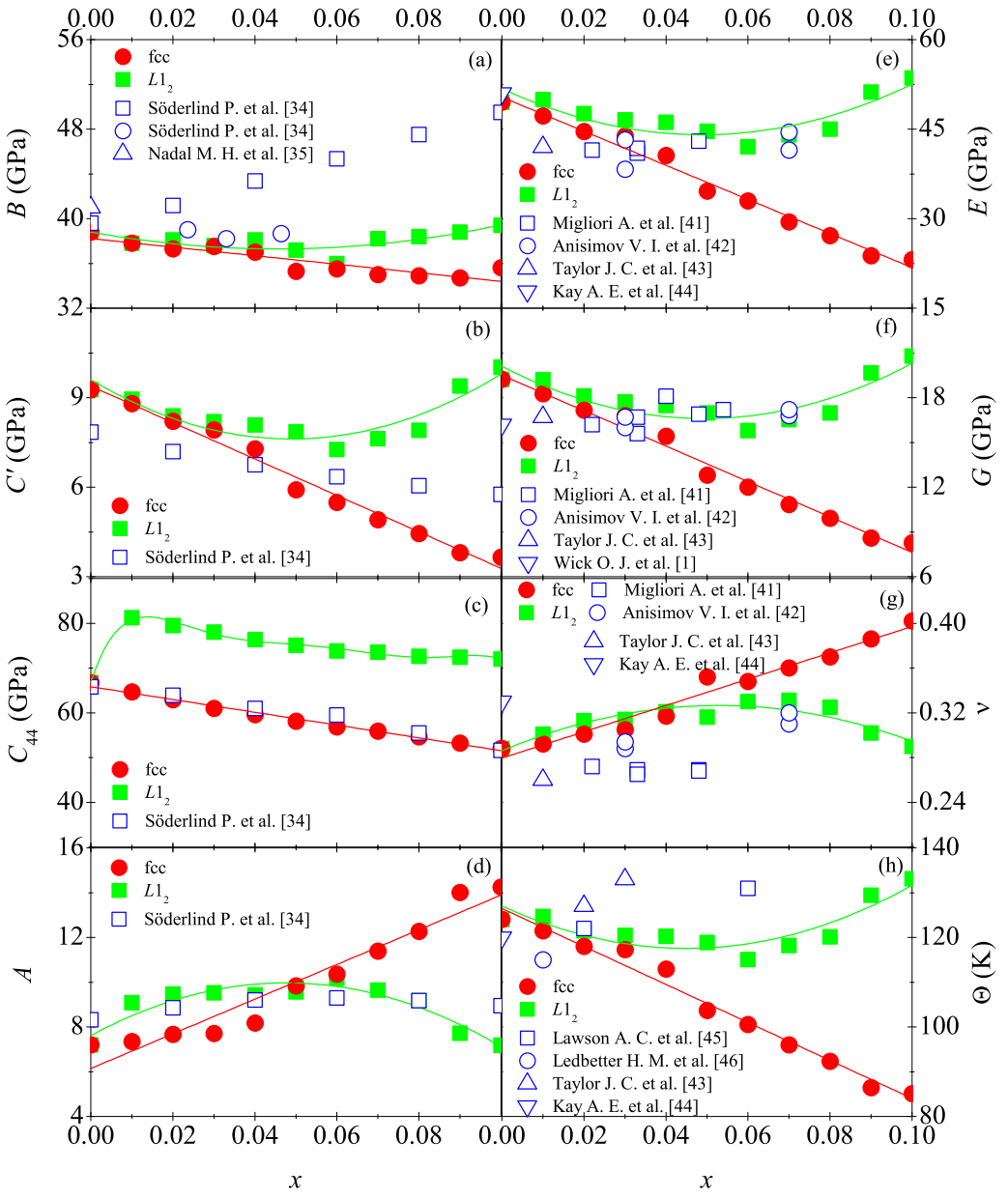

FIG. 4. x dependence of the 0-K bulk modulus (B), shear elastic constants (C' and C_{44}), elastic anisotropy ($A = C_{44}/C'$), Young modulus (E), shear modulus (G), Poisson ratio (ν), and Debye temperature (Θ) of δ-$Pu_{1-x}Ga_x$ ($0 \leqslant x \leqslant 0.1$) alloys with the fcc and $L1_2$ structures, respectively, in comparison with the available experimental and theoretical results from Refs. [1,34,35,41–46].

results according to Vegard's law in the two groups of alloys. In comparison, the lattice collapse with the M addition is shown more evidently in M = Ga than M = Al alloys.

C. Elastic properties

The 0-K B, C', C_{44}, elastic anisotropy ($A = C_{44}/C'$), Young modulus (E), shear modulus (G), Poisson ratio (ν), and Debye temperature (Θ) of δ-$Pu_{1-x}Ga_x$ ($0 \leqslant x \leqslant 0.1$) with the fcc and $L1_2$ structures, respectively, are shown as a function of x in Fig. 4. For the single-crystal elastic constants, the B, C', and C_{44} of the fcc structure decrease linearly with increasing x. In the $L1_2$ structure, both the B and C' first decrease and then increase with x above $x = 0.07$, whereas the C_{44} can quickly get stiffen around $x = 0.01$ and then slowly get soften with further increasing x. The variation of A with respect to x is right contrary to the trend of C' versus x of both the fcc and $L1_2$ structures. The above trends of $C' \sim x$ and $C_{44} \sim x$ of the fcc structure, and that of $A \sim x$ of the $L1_2$ structure tend to be in line with the previous EMTO results [34]. Nevertheless, the variation of B versus x of both the fcc and $L1_2$ structures seem to be a little far away from the previous EMTO calculations, which gave the B fast going up with x [34]. Furthermore, by extending the curves of experimental $B \sim T$ for $x = 0$, 0.0236, 0.0330, and 0.0464 to 0 K [34,35], we approximately get the experimental B values for these four compositions at 0 K. It is found that our present B values of the two structures are in agreement with these four expended data.

Shown in Fig. 4, the estimated E, G, and Θ of the fcc structure decrease linearly with increasing x, whereas in the

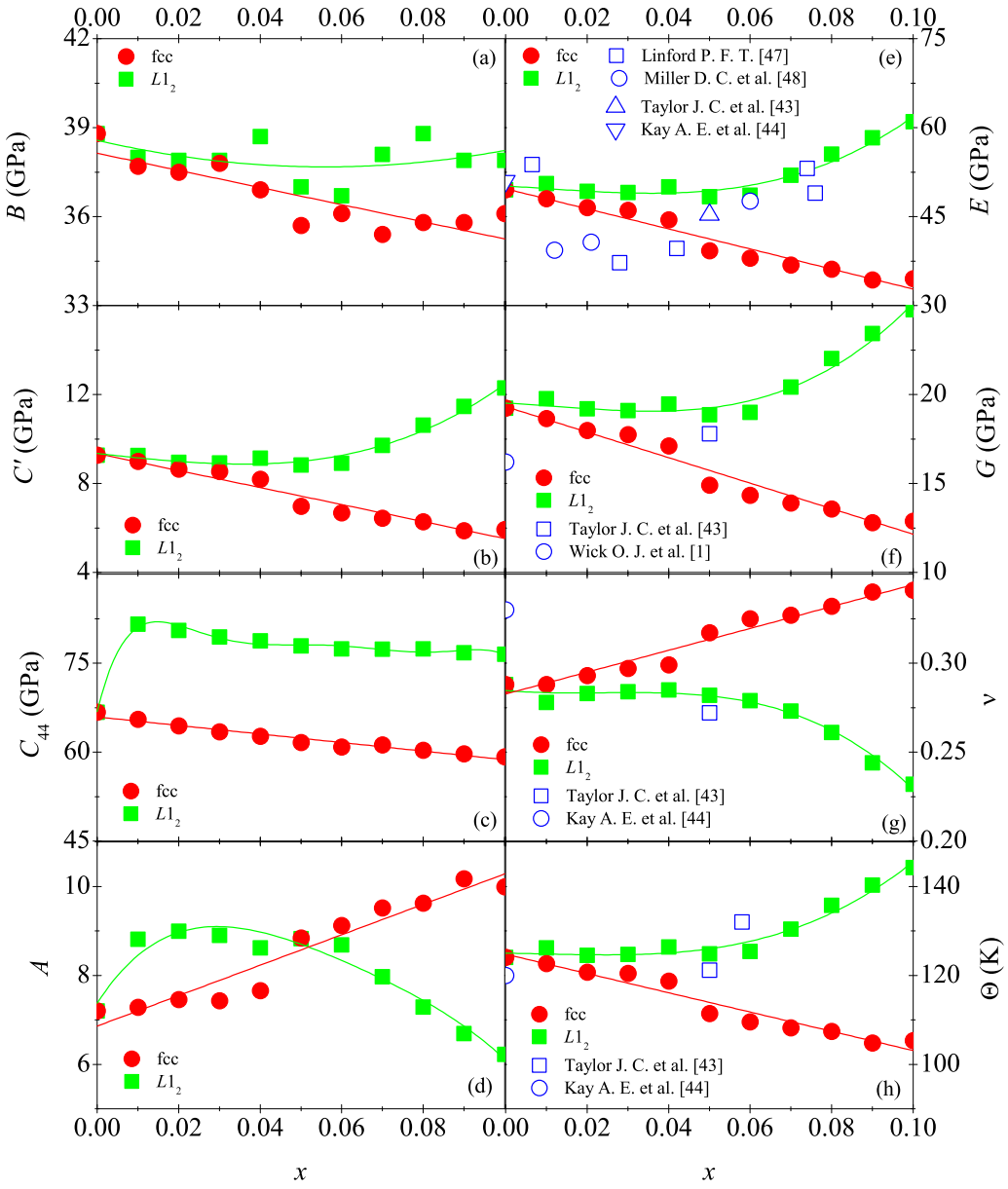

FIG. 5. x dependence of the 0-K bulk modulus (B), shear elastic constants (C' and C_{44}), elastic anisotropy ($A = C_{44}/C'$), Young modulus (E), shear modulus (G), Poisson ratio (ν), and Debye temperature (Θ) of δ-$Pu_{1-x}Al_x$ ($0 \leqslant x \leqslant 0.1$) alloys with the fcc and $L1_2$ structures, respectively, in comparison with the available experimental and theoretical results from Refs. [1,43,44,47,48].

$L1_2$ structure, they first decrease and then increase with x above $x = 0.07$. The calculated $\nu \sim x$ of the two structures just do so in a contrary manner with them. For $x \leqslant 0.04$, the static E, G, ν, and Θ values of the fcc and $L1_2$ structures are similar at each x, and all of them are comparable with the available experimental data shown in Fig. 4 [1,41–46]. For $x > 0.04$, their differences between the two structures get more and more large with the Ga addition. This results that the values corresponding to the $L1_2$ structure are still close to the experimental ones [41,42,45], whereas those of the fcc structure are more and more far away from these measured data with increasing x there. From the mechanical point of view, it is indicated again that for $x \leqslant 0.04$, the fcc and $L1_2$ structures coexist, whereas above $x = 0.04$, the $L1_2$ structure is gradually stabilized alone with the Ga addition in δ-$Pu_{1-x}Ga_x$ alloys.

In Fig. 5, the trends of these above static elastic constants versus x of δ-$Pu_{1-x}Al_x$ with both the fcc and $L1_2$ structures are shown. For the fcc structure, the obtained x-dependence of these elastic constants are similar to those corresponding to δ-$Pu_{1-x}Ga_x$ in Fig. 4. Some small differences present in the $L1_2$ structure, where all the C', E, G, ν, and Θ of $M =$ Al alloys tend to keep a constant below $x = 0.07$ [shown in Figs. 5(b), 5(e), 5(f), 5(g), and 5(h)], whereas in $M =$ Ga alloys they change almost linearly with increasing x for $x \leqslant 0.07$ [shown in Figs. 4(b), 4(e), 4(f), 4(g), and 4(h)]. Besides, in the $L1_2$ structure, the maximum of A of $M =$ Al alloys appears around $x = 0.02$ [shown in Fig. 5(d)] whereas in $M =$ Ga alloys, it is about $x = 0.05$ [shown in Fig. 4(d)]. In Fig. 5, for $x \leqslant 0.04$, the estimated E values of both the fcc and $L1_2$ $Pu_{1-x}Al_x$ alloys tend to be comparable with

TABLE I. Resolved average slopes of these static elastic constants versus x of the fcc $Pu_{1-x}M_x$ (M = Ga and Al, $0 \leqslant x \leqslant 0.1$) alloys: bulk modulus ($\frac{dB}{dx}$, in GPa), shear elastic constants ($\frac{dC'}{dx}$ and $\frac{dC_{44}}{dx}$, in GPa), elastic anisotropy ($\frac{dA}{dx}$), Young modulus ($\frac{dE}{dx}$, in GPa), shear modulus ($\frac{dG}{dx}$, in GPa), Poisson ratio ($\frac{d\nu}{dx}$), and Debye temperature ($\frac{d\Theta}{dx}$, in K).

Alloys	$\frac{dB}{dx}$	$\frac{dC'}{dx}$	$\frac{dC_{44}}{dx}$	$\frac{dA}{dx}$	$\frac{dE}{dx}$	$\frac{dG}{dx}$	$\frac{d\nu}{dx}$	$\frac{d\Theta}{dx}$
$Pu_{1-x}Ga_x$	−38.3	−61.1	−142.9	77.5	−285.8	−118.8	1.18	−424.5
$Pu_{1-x}Al_x$	−28.9	−38.2	−72.0	34.2	−169.1	−71.8	0.61	−216.7

these measured data [44,47,48]. Nevertheless, for $x > 0.04$, all the E, G, ν, and Θ values of the $L1_2$ structure are close to the available experimental ones [43,47,48], whereas those of the fcc structure are more and more far away from these measured data with the increase of x. In the δ-$Pu_{1-x}Al_x$ alloys, the fcc and $L1_2$ structures also tend to co-exist for $x \leqslant 0.04$, whereas when $x > 0.04$, the $L1_2$ structure is gradually stabilized alone with the Al addition.

In Table I, the resolved average slopes of these elastic constants versus x of the fcc $Pu_{1-x}Ga_x$ are compared with those of the fcc $Pu_{1-x}Al_x$. It is found that all the slopes of $B \sim x$, $C' \sim x$, $C_{44} \sim x$, $E \sim x$, $G \sim x$, and $\Theta \sim x$ turn out to be negative whereas those of $A \sim x$ and $\nu \sim x$ are positive, indicating that the elastic stability of these alloys will get to be worse and worse with the M addition. In their absolute values, these slopes corresponding to the fcc $Pu_{1-x}Ga_x$ are always much larger than those to the fcc $Pu_{1-x}Al_x$. Moreover, shown in Fig. 4, at each x, the elastic moduli of both the fcc and $L1_2$ $Pu_{1-x}Ga_x$ tend to be a little smaller than those corresponding to $Pu_{1-x}Al_x$ in Fig. 5. In comparison with the Al doping, the Ga addition brings a greater destruction to the mechanical stability of δ-Pu,

D. Electronic structure

$Pu_{0.93}Ga_{0.07}$ and $Pu_{0.97}Al_{0.03}$ have been confirmed to be energetically most favorable compositions for the fcc Ga and Al adopted alloys, respectively, at 0 K. With their determined equilibrium volumes, we calculate the static DOS of the two alloys with the fcc as well as $L1_2$ structure, and especially compare these partial DOS (PDOS) of Pu in the fcc, Pu1 and Pu2 in the $L1_2$, and M in both the fcc and $L1_2$ structures of the two alloys with that of δ-Pu. As shown in Figs. 6 (M = Ga) and 7 (M = Al), there is a dominated peak in the DOS of the s, d, and f states, respectively, whereas two small peaks appear in the DOS of the p state for all these atoms, denoted by the arrows. Corresponding to each state, all these peaks are shown around almost similar energy below the Fermi level, indicating that the electronic hybridization between Pu and M atoms may exist in all the s, p, d, and f states. For the s, d, and f states, the peaks of Pu atoms are greater than those of M atoms in each system. For the p state, nevertheless, the two small peaks of M atoms turn out to be bigger than those of all Pu atoms in any alloy. The interactions between Pu and M atoms may be thus dominated by Pu for the s, d, and f states but M atoms for the p state. As a result, with Pu replacing with Ga/Al in the fcc $Pu_{0.93}Ga_{0.07}$/$Pu_{0.97}Al_{0.03}$, the big peaks corresponding to the s, d, and f states of Pu atoms get smaller, whereas the two small

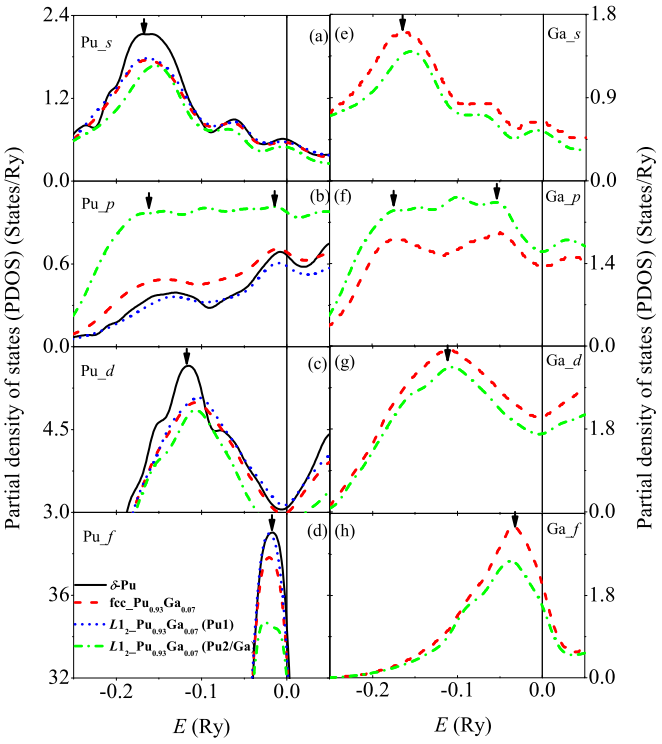

FIG. 6. Partial density of states (PDOS) of Pu in the fcc, Pu1 and Pu2 in the $L1_2$, and Ga of the two structures of $Pu_{0.93}Ga_{0.07}$ are compared with that of δ-Pu. The arrows denote the dominated peaks shown in each of these PDOS, and the vertical lines indicate the Fermi level.

peaks of their p state are bigger than those of δ-Pu. The similar results are also found for Pu2 atoms in the $L1_2$ alloys, which co-occupy the same sublattice with M atoms as well as Pu atoms in the fcc alloys. Shown in Figs. 6 and 7, in comparison with δ-Pu, the changes in the PDOS of Pu2 atoms in the $L1_2$ alloys are greater than those in the PDOS of Pu atoms in the fcc alloys, indicating that the interactions between Pu2 and M atoms in the $L1_2$ structure should be stronger than those between Pu and M in the fcc structure for each composition.

For Pu1 atoms in the $L1_2$ structure, which occupy one sublattice alone, their DOS of the s and d states are similar to those corresponding to Pu atoms in the fcc structure, whereas in the p and f states, their DOS are comparable with those of δ-Pu, as shown in Figs. 6 and 7. It reflects that the electronic hybridization between Pu1 and M atoms is even weaker than that between Pu and M atoms in the fcc structure. In the alloys with $x > 0.04$, the relative stability of the $L1_2$ to the fcc structure should be thus ascribed to the strong interactions between Pu2 and M atoms in the $L1_2$ structure. Shown in Fig. 6, the difference of PDOS between Pu2/M in the $L1_2$ and Pu/M in the fcc $Pu_{0.93}Ga_{0.07}$ is a little larger than that of $Pu_{0.97}Al_{0.03}$ in Fig. 7. In a large degree it indicates that with increasing x, the $L1_2$ structure will get more and more stable than the fcc one.

Finally, we calculate the smeared DOS and then E_f^* of all the δ-$Pu_{1-x}M_x$ (M = Ga and Al, $0 \leqslant x \leqslant 0.1$) alloys with both the fcc and $L1_2$ structures at electronic temperature T = 700 K. Shown in the insert figures of Figs. 8(a) and 8(b),

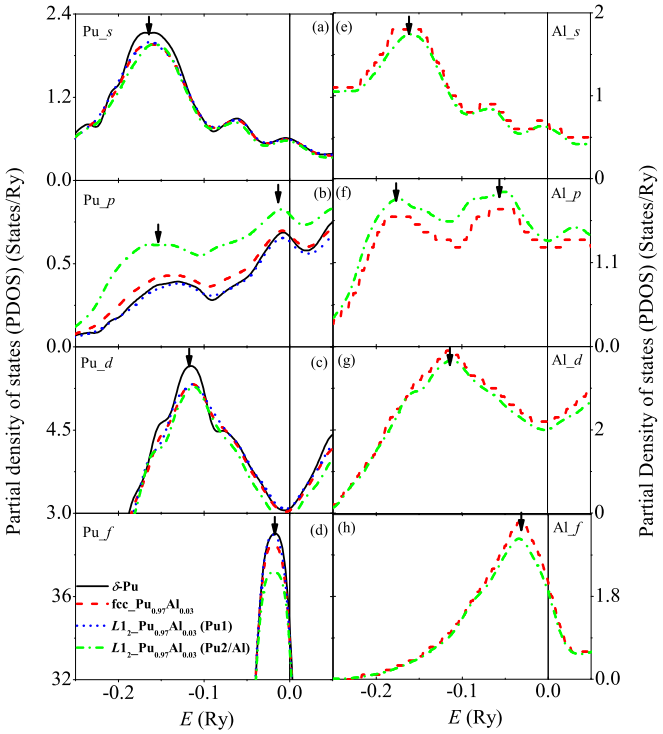

FIG. 7. Partial density of states (PDOS) of Pu in the fcc, Pu1 and Pu2 in the $L1_2$, and Al of the two structures of $Pu_{0.97}Al_{0.03}$ are compared with that of δ-Pu. The arrows denote the dominated peaks shown in each of these PDOS, and the vertical lines indicate the Fermi level.

respectively, the differences between the E_f^* and E_f ($\Delta E_f = E_f^* - E_f$), with positive values, increase with x in each structure of M = Ga and Al alloys. It is mainly ascribed that the differences between the E_{el}^* and E_{el}($\Delta E_{el} = E_{el}^* - E_{el}$)

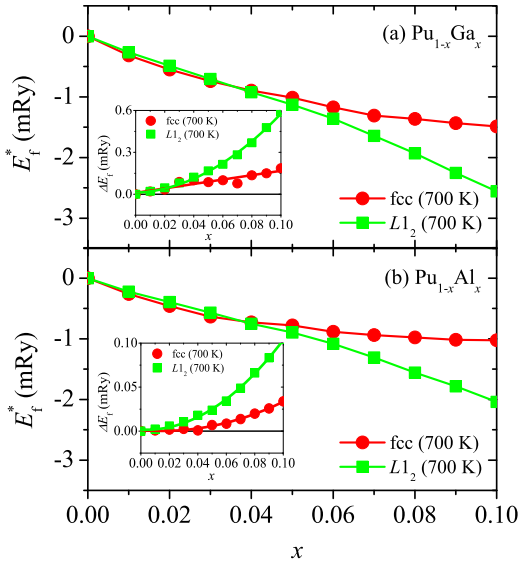

FIG. 8. x-dependence of the smeared formation energies (E_f^*) of δ-$Pu_{1-x}M_x$ [M = Ga (a) and Al (b), $0 \leqslant x \leqslant 0.1$] with the fcc and $L1_2$ structures, respectively, at 700 K. In the two insert figures, the difference between the smeared and static formation energies ($\Delta E_f = E_f^* - E_f$) of the two structures of these alloys at 700 K are especially shown with respect to x in detail.

are big and with negative values, they increase with x as well in each group of alloys. Nevertheless, the differences between the $-TS_{el}^*$ and $-TS_{el}$ [$-T\Delta S_{el} = -T(S_{el}^* - S_{el})$] are relative small and with positive values, they do not change very much with the increase of x. As a result, shown in Figs. 8(a) and 8(b), the calculated E_f^* is a little larger than the E_f in Figs. 2(a) and 2(b) for each binary alloy, whereas the trend of $E_f^* \sim x$ is similar to the corresponding that of $E_f \sim x$. At finite temperature, the electron-phonon coupling further decreases the phase stability of δ-$Pu_{1-x}M_x$ a little bit, and with increasing x, their stability will get worse and worse due to the reduce of the strong-correlated Pu atoms.

IV. SUMMARY

Using first-principles EMTO-CPA method, we have systematically investigated the composition-dependent crystal structure, volume, elastic constants, and electronic structure of δ-$Pu_{1-x}M_x$ (M = Ga and Al, $0 \leqslant x \leqslant 0.1$) alloys. The main results are summarized as follows.

(1) In the alloys with $x \leqslant 0.04$, the fcc and $L1_2$ structures tend to co-exist whereas for $x > 0.04$, the $L1_2$ structure gets to be both energetically and mechanically more and more stable than the fcc one with increasing x, and around $x = 0.1$, it is expected to be stabilized alone.

(2) The calculated V of both the fcc and $L1_2$ alloys decrease monotonically with increasing x, which, as well as the experimental $V \sim x$, are negative deviation from Vegard's law. However, only with the $L1_2$ structure, the V going down against x is faster in $Pu_{1-x}Ga_x$ than $Pu_{1-x}Al_x$, which is in line with the measured result.

(3) All the evaluated C', E, G, and Θ decrease linearly with increasing x in the fcc alloys, whereas in the $L1_2$ alloys, they suddenly change to increase with x above $x = 0.07$. The calculated $\nu \sim x$ of both the fcc and $L1_2$ alloys just do so in a contrary manner with them. For $x \leqslant 0.04$, the estimated elastic moduli of the two structures are in agreement with the experimental data whereas for $x > 0.04$, only those of $L1_2$ structure are close to the experimental results.

(4) The electronic hybridization between Pu and M atoms exists in all the s, p, d, and f states, dominated by Pu atoms for the s, d, and f states but M atoms for the p state. The strong interactions between Pu2 and M atoms in the $L1_2$ structure should be responsible for its relative stability in the alloys with $x > 0.04$. The electron-phonon coupling further decreases the phase stability of δ-$Pu_{1-x}M_x$ with increasing x at finite temperature.

ACKNOWLEDGMENTS

The authors acknowledge the financial support from the NSFC under Grants No. 51271181, No. 51301176, and No. 11674233, and the MoST of China under Grant No. 2014CB644001. The China postdoctoral Science Foundation as well as Liaoning Province Science Foundation is acknowledged for financial support. Chun-Mei Li is also grateful to the T. S. Kê Research Fellowship of IMR/SYNL.

[1] O. J. Wick, *Plutonium Handbook: A Guide to the Technology* (Gordon and Breach, New York, 1967).
[2] R. C. Albers, Nature (London) **410**, 759 (2001).
[3] M. Ling, R. F. E. Jenkins, and N. Park, J. Alloys Compd. **586**, 709 (2014).
[4] S. S. Hecker, D. R. Harbur, and T. G. Zocco, Prog. Mater. Sci. **49**, 429 (2004); Metall. Mater. Trans. A **35**, 2207 (2004).
[5] R. C. Albers and J. X. Zhu, Nature (London) **446**, 504 (2007).
[6] *Challenges in Plutonium Science*, Los Alamos Science Vol. 26, edited by N. G. Cooper (Los Alamos National Laboratory, Los Alamos, 2000).
[7] L. E. Cox, R. Martinez, J. H. Nickel, S. D. Conradson, and P. G. Allen, Phys. Rev. B **51**, 751 (1995).
[8] P. Faure, B. Deslandes, D. Bazin, C. Tailland, R. Doukhan, J. M. Fournier, and A. Falanga, J. Alloys Compd. **244**, 131 (1996).
[9] O. J. Wick, *Plutonium Handbook: A Guide to the Technology* (American Nuclear Society, La Grange Park, IL, 1980), p. 966.
[10] F. H. Ellinger, C. C. Land, and W. N. Miner, J. Nucl. Mater. **5**, 165 (1962).
[11] A. J. Schwartz, H. Cynn, K. J. M. Blobaum, M. A. Wall, K. T. Moore, W. J. Evans, D. L. Farber, J. R. Jeffries, and T. B. Massalski, Prog. Mater. Sci. **54**, 909 (2009).
[12] G. Robert, A. Pasturel, and B. Siberchicot, Phys. Rev. B **68**, 075109 (2003).
[13] P. H. Adler, Metall. Trans. A **22**, 2237 (1991).
[14] S. D. Conradson *et al.*, Phys. Rev. B **89**, 224102 (2014).
[15] P. Soderlind, F. Zhou, A. Landa, and J. E. Klepeis, Sci. Rep. **5**, 15958 (2015).
[16] M. Janoschek, P. Das, B. Chakrabarti, D. L. Abernathy, M. D. Lumsden, J. M. Lawrence, J. D. Thompson, G. H. Lander, J. N. Mitchell, S. Richmond, M. Ramos, F. Trouw, J. X. Zhu, K. Haule, G. Kotliar, and E. D. Bauer, Sci. Adv. **1**, e1500188 (2015).
[17] P. Söderlind, A. Landa, and B. Sadigh, Phys. Rev. B **66**, 205109 (2002).
[18] A. Landa, P. Söderlind, and A. Ruban, J. Phys.: Condens. Matter **15**, L371 (2003).
[19] P. Söderlind and B. Sadigh, Phys. Rev. Lett. **92**, 185702 (2004).
[20] J. C. Lashley, A. Lawson, R. J. McQueeney, and G. H. Lander, Phys. Rev. B **72**, 054416 (2005).
[21] J. Staunton, B. L. Gyoffy, A. J. Pindor, G. M. Stocks, and H. Winter, J. Magn. Magn. Mater. **45**, 15 (1984).
[22] A. Solontsov and V. P. Antropov, Phys. Rev. B **81**, 214402 (2010).
[23] O. K. Andersen, O. Jepsen, and G. Krier, in *Lectures on Methods of Electronic Sutructure Calculations*, edited by V. Kumar, O. K. Andersen, and A. Mookerjee (World Scientific, Singapore, 1994), pp. 63–124.
[24] L. Vitos, *Computational Quantum Mechanics for Materials Engineers* (Springer-Verlag, London, 2007).
[25] L. Vitos, I. A. Abrikosov, and B. Johansson, Phys. Rev. Lett. **87**, 156401 (2001).
[26] P. Soven, Phys. Rev. **156**, 809 (1967).
[27] B. L. Györffy, Phys. Rev. B **5**, 2382 (1972).
[28] L. Vitos and B. Johansson, Phys. Rev. B **79**, 024415 (2009).
[29] Z. H. Dong, W. Li, S. Schönecker, S. Lu, D. F. Chen, and L. Vitos, Phys. Rev. B **92**, 224420 (2015).
[30] D. Y. Kim, J. Hong, and L. Vitos, Phys. Rev. B **90**, 144413 (2014).
[31] J. P. Perdew, K. Burke, and M. Ernzerhof, Phys. Rev. Lett. **77**, 3865 (1996).
[32] V. L. Moruzzi, J. F. Janak, and K. Schwarz, Phys. Rev. B **37**, 790 (1988).
[33] C. M. Li, Q. M. Hu, R. Yang, B. Johansson, and L. Vitos, Phys. Rev. B **82**, 094201 (2010).
[34] P. Söderlind, A. Landa, J. E. Klepeis, Y. Suzuki, and A. Migliori, Phys. Rev. B **81**, 224110 (2010).
[35] M. H. Nadal and L. Bourgeois, J. Appl. Phys. **108**, 073532 (2010).
[36] G. Grimvall, *Thermophysical Properties of Materials* (North-Holland, Amsterdam, 1999)
[37] M. J. Graf, T. Lookman, J. M. Wills, D. C. Wallace, and J. C. Lashley, Phys. Rev. B **72**, 045135 (2005).
[38] F. H. Ellinger, C. C. Land, and V. O. Strauebing, J. Nucl. Mater. **12**, 226 (1964).
[39] R. O. Elliott, K. A. Gschneidner, and C. P. Kempter, *Plutonium 1960*, (Cleaver-Hume, London, 1961), p. 142.
[40] J. Wong, M. Krisch, D. L. Farber, F. Occelli, A. J. Schwartz, T.-C. Chiang, M. Wall, C. Boro, and R. Xu, Science **301**, 1078 (2003).
[41] A. Migliori, I. Mihut, J. B. Betts, M. Ramos, C. Mielke, C. Pantea, and D. Miller, J. Alloys Compd. **444-445**, 133 (2007).
[42] V. I. Anisimov, V. V. Dremov, M. A. Korotin, G. N. Rykovanov, and V. V. Ustinov, Phys. Met. Metallogr. **114**, 1087 (2013).
[43] J. C. Taylor, P. F. T. Linford, and D. J. Dean, J. Inst. Metals. **96**, 178 (1968).
[44] A. E. Kay and R. G. Loasby, Philos. Mag. **9**, 37 (1964).
[45] A. C. Lawson, B. M. Artinez, J. A. Roberts, B. I. Bennett, and J. W. Richardson Jr., Philos. Mag. B **80**, 53 (2000); A. C. Lawson, J. A. Roberts, B. Martinez, M. Ramos, G. Kotliar, F. W. Trouw, M. R. Fitzsimmons, M. P. Hehlen, J. C. Lashley, H. Ledbetter, R. J. Mcqueeney, and A. Migliori, Philos. Mag. **86**, 2713 (2006).
[46] H. M. Ledbetter and R. L. Moment, Acta Metall. **24**, 891 (1976).
[47] P. F. T. Linford, Private Communication, reported by H. R. Gardner, in Chap. 4, *The Plutonium Handbook*, 1966.
[48] D. C. Miller and J. S. White, J. Nucl. Mater. **10**, 339 (1963).